

Development of a Hybrid Vehicular Prototype with H₂/air PEMFC Stack and Li-Ion Battery Module

José Luis Díaz-Bernabé*, Andrés Rodríguez-Castellanos, Sebastián Citalán-Cigarroa, Israel Arenas-Mendoza, Omar Solorza-Feria

Departamento de Química, Centro de Investigación y de Estudios Avanzados del IPN, Av. Instituto Politécnico Nacional 2508, Sn. Pedro Zacatenco, 07360, CDMX, México.

*Corresponding author: José Luis Díaz-Bernabé, email: jldiaz@cinvestav.mx, Phone: 55-5747-3800 ext. 4416.

Received February 24th, 2023; Accepted May 30th, 2023.

DOI: <http://dx.doi.org/10.29356/jmcs.v67i4.1987>

This paper is in honor of Dr. Omar Solorza-Feria as an electrochemical member of emeritus researcher of the Mexican National System of Researchers, SNI.

Abstract. Recent years have marked a huge increase in worldwide efforts to improve the design and manufacture of miniaturized low- and high- power Polymer Electrolyte Membrane Fuel Cells (PEMFCs) for diverse electronic applications, ranging from stationary backup power to mobile transportation, and even as energy sources for a new generation of drone and hybrid vehicular transportation technologies. This communication compiles recent contributions developed by our group of researchers who has worked in the synthesis and characterization of Pt-based catalysts for oxygen reduction reaction (ORR) and in to address the performance and durability of H₂/O₂ PEMFC - Li Ion batteries in an electric vehicular transport prototype. We will provide an overview of our current contributions in the design, manufacturing, and development of low temperature, high-energy H₂/O₂ fuel cells which generated electricity is storage in a set of Li-Ion batteries for a vehicular transport prototype, Cinvestav-Sicarú, with more than an hour and thirty minutes of autonomy.

Keywords: H₂/O₂ PEMFC energy sources; hydrogen catalysts; FCHEV powertrain performance.

Resumen. Los últimos años han marcado un aumento sustancial en los esfuerzos mundiales para mejorar el diseño y la fabricación de celdas de combustible de membrana de electrolito de polímero (PEMFC) miniaturizadas de baja y alta potencia para diversas aplicaciones electrónicas, que van desde energía de respaldo estacionaria hasta transporte móvil, e incluso como energía. Fuentes para una nueva generación de tecnologías de transporte de drones y vehículos híbridos. Este trabajo recopila contribuciones recientes desarrolladas por nuestro grupo de investigación que ha trabajado en la síntesis y caracterización de catalizadores basados en Pt para la reacción de reducción de oxígeno (ORR) y para abordar el rendimiento y la durabilidad de una celda de combustible H₂/O₂ – banco de baterías de Iones de litio en un prototipo de transporte vehicular eléctrico. Proporcionaremos una descripción general de nuestros desarrollos actuales en el diseño, fabricación y desarrollo de celdas de combustible H₂/O₂ de alta energía y baja temperatura que generan electricidad y se almacenan en un conjunto de baterías de iones de litio para un prototipo de transporte vehicular, con más de una hora y media de autonomía.

Palabras clave: Fuentes de energía de H₂/O₂; catálisis del hidrógeno; funcionamiento del tren de potencia de un FCHEV.

Introduction

Recent studies reflected the growing consensus that it will be inevitable to initiate and accelerate the energy transition from traditional energy systems to innovative and sustainable alternatives. The integration of energy systems with the coupling of clean sources to produce electricity represents a solution to problems related to environmental pollution, climate change, damage to health and energy supply. In recent decades, the direct conversion of chemical energy to electrical energy via fuel cells has been the focus of electrochemical research and technological developments. The interest in studying fuel cells rests fundamentally on two factors: the high efficiencies in energy conversion, and the noticeable decrease in pollutants emitted into the atmosphere. Fuel cell technology requires an interdisciplinary involvement, which ranges from the use of different fuels, mainly hydrogen, and its processing, through knowledge of basic concepts in electrochemistry, chemical and mechanical engineering, and automatic control systems [1]. Hydrogen, a clean energy source with the highest specific energy density, represents the best alternative to batteries and fossil fuels used in conventional energy production [2-4]. Efforts are still being made to improve the performance of Fuel cell hybrid electric vehicle (FCHEV) prototypes as powertrain layout, PEMFC system integration, and energy management strategy solutions among others as the developments reported in [5-8]. In [5] a 10 kW PEMFC system was developed and tested for a five-seater small car using a hydrogen tank type III. In this communication we present the design, manufacture, and performance results of a fuel cell hybrid electric vehicle prototype (FCHEV), H₂/O₂ PEMFC along with Li-ion batteries, considering reliability and sizing space and taking into consideration that the use of this technology reduces to zero the pollutants into the environment. The work is organized as follows: Section II describes the design methodology for the chassis, powertrain, PEMFC stack, and battery module. Section III presents the development of the prototype, and the experimental behavior of the powertrain at a suitable speed cycle for small vehicles. Finally, conclusions are given in section IV.

Development of the FCHEV prototype

Chassis building

The chassis design, proposed using computer aid design (CAD) methods, was conceived for three passengers, the front driver, and passengers, as well as for a person in a wheelchair and a rear passenger in back. Fig. 1(a)-1(d) shows several computer design sights produced in Solid-works software [9-10] and Fig. 1(e) shows a structural deformation simulation carried out by ANSYS Workbench platform with finite element analysis (FEA) against a frontal collision at a velocity of 50 km/h as reported in [11-13]. The body of the prototype was projected to be made of round tube aluminium alloy type 6063-T6 with 33.4 mm external diameter and 26.64 mm internal diameter.

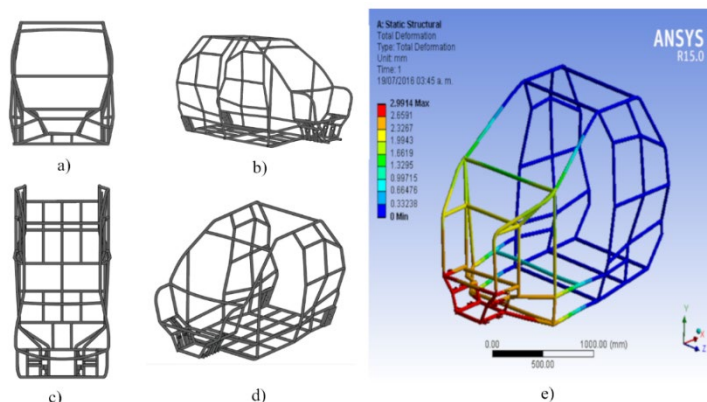


Fig. 1. Computer design and simulation of chassis. (a) front view; (b) right-frontal view; (c) top view; (d) left-frontal view; (e) Structure deformation and stress against a frontal impact with ANSYS simulation.

PEMFC design

The design of PEMFC stack is based on a numerical modelling developed by our research group, [14]. An algorithm developed in Java combines stoichiometric calculations for the reaction $2\text{H}_2 + \text{O}_2 \rightarrow 2\text{H}_2\text{O}$ [15-16] and the Ohm's law for the electric circuit calculations. Required input parameters include power, current collector plate, and output voltage among others. The output results are the number of current collector plates, effective area of plates, maximum and optimized values of power, voltage, and current, the expected volume and weight of PEMFC stack, and the expected consumption of H_2 and air, see Fig. 2(a). The bipolar plates are made of good conductor high resistivity graphite, with a channel pattern that facilitates the gas flow on each face of the electrodes. At the same time, they make electrical contact with the surface of each alternate electrode. A computer numerical control (CNC) milling machine with an optimized channel pattern program was employed to fabricate polar, bipolar, and final plates, see Fig. 2(b). The PEMFC stack was fixed with forty-eight membrane-electrodes, MEAs, in a single cell with an electrode surface geometric area of 123 cm^2 for anode and cathode sides. This configuration creates a stack that feeds serpentine channels to feed humidified air-dry hydrogen and horizontal channels to feed air above the cathode. Fig. 2(c) shows a compact PEMFC stack arrangement which benefits the electric current flow. The edges of the electrodes are sealed with silicone gaskets, also around each MEA to avoid short-circuit in between them. The PEMFC stack dimensions are 26 cm large, 8 cm wide, and 20 cm high.



Fig. 2. PEMFC development. (a) PEMFC numerical modeling [10]; (b) Bipolar plates with serpentine; (c) PEMF stack assembly.

Li-Ion battery sizing

Li-ion cells are the most widespread technology in EV's because of their small size, high current density, and availability [17-18]. Containing a grid of N_s serial connected and N_p parallel connected cells, battery module increases the charge storage capacity, the discharging current, and the open-circuit voltage of a single small Li-Ion cell. The battery module should be sized for the expected vehicle cruiser velocity as the installed electric motor power size for the specific drive-cycle. As mentioned in [19] an early estimation of the required electric power for an HEV is approximated by the equation (1):

$$P \geq \frac{V}{1000\eta_t\eta_m} \left(Mg f_r + \frac{1}{2} \rho_a C_d A_f V^2 \right) \quad (1)$$

where V is the velocity, M is the mass, f_r is the friction coefficient, ρ_a is the humidity factor, A_f is the drag coefficient, η_t is the transmission ratio (wheel radius to motor-shaft ratio), and η_m is the efficiency of the motor. Once the module power requirement is estimated, module voltage v_b should correspond to the nominal supply voltage v_s of the motor-drives and the module discharge-current i_b might increase as the expected autonomy in

hours. As described in [17], module voltage and discharge-current determine the series cell number N_s per string and the parallel string number N_p respectively of the projected Li-Ion battery module by:

$$N_s = \frac{v_b}{v_c} \quad (2)$$

$$N_p = \frac{i_b}{i_c} \quad (3)$$

where v_c and i_c are the nominal voltage and current of a single Li-Ion cell.

FCHEV Powertrain

Fig. 3 shows the simplified diagram of a series powertrain for FCHEV [20]. The structure includes a PEMFC stack and a switch-mode DC-DC converter as power conditioning unit (PCU), Li-Ion battery module, motor-drive, brushless direct-current (BLDC) motor, transmission ratio, and vehicle body dynamics. An energy management strategy (EMS) schedules the PEMFC energy source and Li-ion battery module to alternatively deliver the supply voltage v_s for motor-drives, see [21-22]. The motor-drive internal speed control loop modifies the motor voltage v_t and takes the angular speed ω close to a velocity command ω_m^* . Comprising speed values versus time, the velocity reference is a drive-cycle or the vehicle driving pattern. It involves well-known periods such as: constant acceleration, constant velocity, brake, and zero speed or a no-movement period. The vehicle body involves mechanical parameters such as weight, speed ratio, rolling force, etc. The instantaneous rolling resistance on wheels acts as load torque τ_L for the BLDC motors.

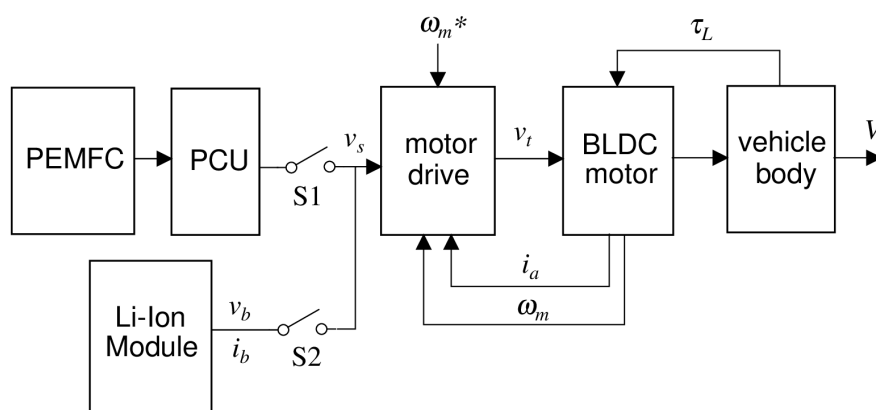


Fig. 3. Simplified series powertrain for FCHEV.

Results and discussion

Fig. 4 shows the Cinvestav FCHEV prototype named Sicarú, made of an aluminum tubular structure taking into consideration frontal impact studies of the entire vehicle body, at a speed of 50 km/h, and it would be absorbed by the impact attenuators as it is shown in Fig. 1(e). The structure measures 270 cm length, 140 cm width, 170 cm height and weighs 280 kg. The external cover of the prototype was made of fiberglass. Table 1 shows other specific body parameters of the developed FCHEV.



Fig. 4. H₂/air PEMFC -Li ion batteries, Cinvestav- Sicarú hybrid electric vehicle.

Table 1. Specifications of FCHEV.

C_d	f_r	A_f (m ²)	Mass (kg)	R_d (m)	Battery (kW)	PEMFC (W)	BLDC Motor
0.3	0.01	1.5	280	0.27	3.7	520	800W,36V

Fig. 5(a) shows the PEMFC stack assembly with auxiliary subsystems, such as cell humidification, air fans for oxygen supply, hydrogen connections, solenoid valve for hydrogen purge, and the electrical main switch. Fig. 5b shows the PEMFC stack voltage against current curve under controlled test conditions with a maximum power point of 520W at 18V, 29A. Table 2 shows the main specifications for the developed PEMFC stack. A 1,400-liter hydrogen tank is installed behind the driver of the prototype vehicle, and the PEMFC stack consumes 520 liter per hour of pure hydrogen per hour.

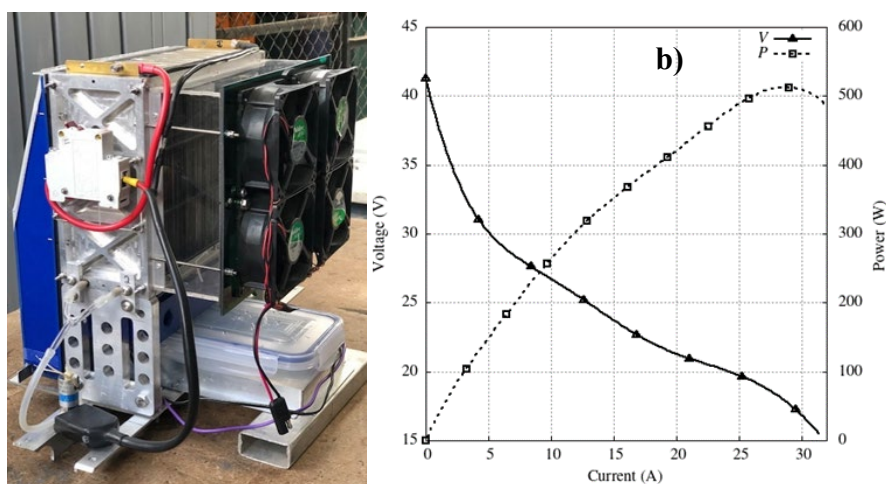


Fig. 5. PEMFC source for HEV. (a) Front view of PEMFC source; (b) Performance under controlled test conditions.

Table 2. Parameters of developed PEMFC source.

Type	N_s	A (cm^2)	J (mA/cm^2)	Power (W)	Material	Reactants	Reactant Pressure (atm)
PEM	48	123	235	520	Pt, 20%	H ₂ , air	0.2

Because Li-Ion cells have high energy density and high availability [18], several 400 cells of the type ICR18650 [23] shape the entire battery module. A 3.7kWh battery module was obtained by means of a configuration of 10 series connected cells and 40 parallel connected cells also known as a 10S40P configuration. Fig. 6(a) shows the *in-situ* Li-Ion module, Fig. 6(b) shows one building block Li-Ion cell formed by 1S40P configuration. Fig. 6(c) shows the theoretical performance carried out by the methodology given in [24]. Table 3 shows the specifications of the battery module.

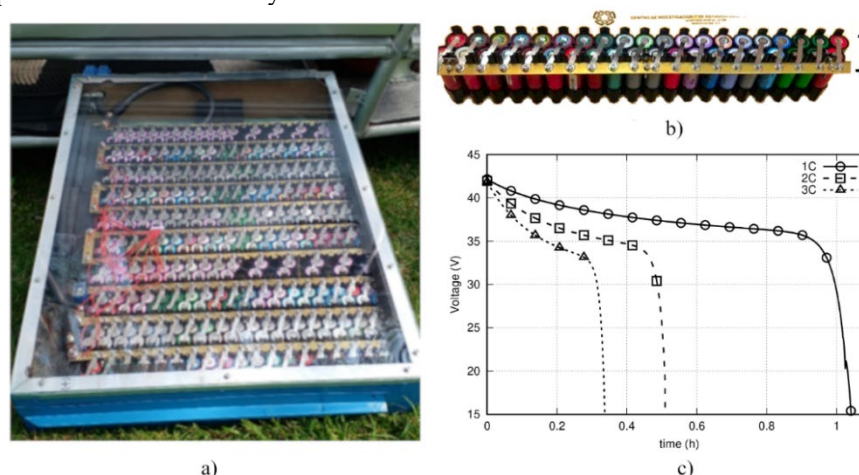


Fig. 6. Li-Ion Battery module. (a) In-situ battery module with a 10S40P configuration; (b) Building block Li-Ion cell with a 1S40P configuration; (c) Expected performance of the Li-Ion battery module.

Table 3. Specifications of the Li-Ion battery module.

Li-Ion Cell			Li-Ion Module			
Type	Nominal Voltage (V)	Nominal Capacity (Ah)	N_s	N_p	Voltage (V)	Energy (kWh)
ICR18650	3.6	2.6	0	0	36	3.7

A four-wheel drive (4wd) powertrain configuration is achieved through a single 800W per wheel BLDC motor. Fig. 7 shows the behavior of the powertrain under a 40 second single drive-cycle. This behavior is described by developing an oscilloscope measurement of the motor-drive current. According to the EMS schedule, the Li-ion battery module must provide the required motor-drive current during the acceleration phase, while the PEMC stack should provide the required current during the cruiser speed phase. The acceleration period lasts ten seconds and its maximum motor-drive current was around 75 A. By the constant velocity lapse, a speed of 25 km/h is reached, and the developed motor-drive current was only 40A. The negative motor-drive current corresponds to the regenerative brake period that returns a small fraction of energy to the supply source. Finally, powertrain holds a zero speed, and no motor-drive current is developed.

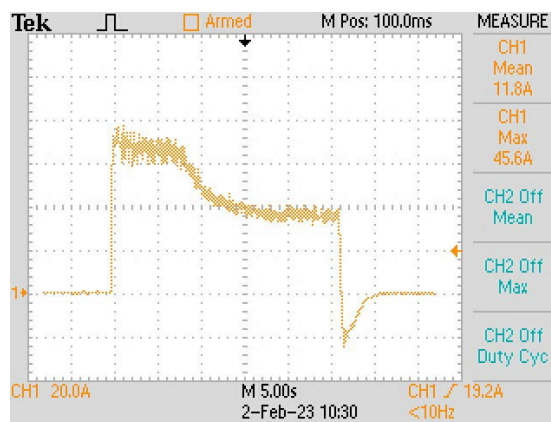


Fig. 7. Measured performance of the FCHEV powertrain under a single drive-cycle.

Conclusions

A hybrid vehicular transport prototype with H₂/air PEMFC and Li-Ion batteries was designed, manufactured, and electrochemically characterized. The PEMFC stack global parameters was estimated by a simple numerical algorithm. CAD tools are used to design and to construct the unipolar and bipolar plates of the PEMFC stack. The parameters of FCHEV were determined for real-time testing of the PEMFC system, battery module, BLDC-motors, vehicle body dynamics, and control algorithms. A Li-Ion battery module was developed, assembled, and tested in our laboratory for a constant current discharge. The performance of the powertrain is characterized under a complete drive-cycle for motor-drive currents. The battery module capacity met the power requirement for FCHEV for maximum velocity of 32 km/h. Battery module and PEMFC stack is an exceptional solution to improve the performance of the FCHEV by enlarging the autonomy of batteries, and by applying a renewable energy source in electric transport. It is expected that in the following years the hybrid electric vehicle prototype grows in Mexico as the beginning of a substantial production of them to reduce the breach with classic gasoline vehicles.

Acknowledgements

This study was financially supported by CINVESTAV and the Mexican National Council of Science and Technology, CONACYT (Grant No. 245920).

References

1. Wu, D.; Yi, C.; Tang, H. *Electrochem. Energy Rev.* **2020**, *51*, 1-40. DOI: <https://doi.org/10.1007/s41918-020-00068-1>.
2. Meloni, E.; Iervolino, G.; Ruocco, C.; Renda, S.; Festa, G.; Martino, M.; Palma, V. *Energies.* **2022**, *15*, 3588-3621. DOI: <https://doi.org/10.3390/en15103588>.
3. Wang, Y.; Ruiz-Diaz D.F.; Chen, K. S.; Wang, Z.; Cordobes, X. *Mater. Today.* **2020**, *32*, 178-203. DOI: <https://doi.org/10.1016/j.mattod.2019.06.005>.
4. Feng, Z.; Huang, J.; Jin, S.; Wang, G.; Chen, Y. J. *Power Sources.* **2022**, *520*, 230808-230823. DOI: <https://doi.org/10.1016/j.jpowsour.2021.230808>.

5. Indian demonstrates hydrogen fuel cell car. *Fuel Cells Bull.* **2020**, 11. DOI: [https://doi.org/10.1016/S1464-2859\(20\)30491-0](https://doi.org/10.1016/S1464-2859(20)30491-0).
6. Katalenich, S. M.; Jacobson, M. Z. *Energy*. **2022**, 254, 124355-124367. DOI: <https://doi.org/10.1016/j.energy.2022.124355>.
7. Cunanan C.; Tran M. -K.; Lee Y.; Kwok, S.; Leung, V.; Fowler, M. *Clean Technol.* **2021**, 3, 474-489. DOI: <https://doi.org/10.3390/cleantechnol3020028>.
8. Bairabathina, S.; Balamurugan S. *Int. J. Hydrogen Energy*. **2020**, 45, 21687- 21713. DOI: <https://doi.org/10.1016/j.ijhydene.2020.05.277>.
9. Lombard M. in: *SolidWorks 2013 Bible*. Ed. John Wiley & Sons, **2013**.
10. Chang, K.-H. in: *Motion Simulation and Mechanism Design with SOLIDWORKS Motion*. Ed. SDC publications, **2021**.
11. Alawadhi, E. M. in: *Finite element simulations using ANSYS*. Ed. CRC Press, **2009**.
12. Enriquez-Miranda M.A. Diseño estructural del chasis por el método de elementos finitos de un transporte biplaza híbrido, que transportará discapacitado en silla de ruedas, funcionando mediante celdas de combustible, 2017, <http://tesis.ipn.mx/handle/123456789/21074>, accessed in September 2023.
13. Rodriguez-Castellanos A. in: *Modelado, Diseño, Construcción y caracterización de una celda de combustible PEM para un dron marca DJI S900*, in SIMEVANT **2018**, Mexico City, Mexico.
14. Li, X. in: *Principles of fuel cells*. Ed. CRC press, **2005**. DOI: <https://doi.org/10.1201/9780203942338>.
15. Barbir F. in: *PEM fuel cells: theory and practice*. Ed. Academic Press, **2012**.
16. Aishwarya, M.; Sailaja, M.; Brisilla R. M. *IEEE i-PACT* **2021**. DOI: <https://doi.org/10.1109/i-PACT52855.2021.9696920>.
17. Sharma S.; Panwar A. K.; Tripathi M. M. *J. Traffic Transp. Eng.* **2020**, 7, 340-361. DOI: <https://doi.org/10.1016/j.jtte.2020.04.004>.
18. Ehsani, M.; Gao, Y.; Longo, S.; Ebrahimi, K. in: *Modern Electric, Hybrid Electric, and Fuel Cell Vehicles*. Ed. CRC press, **2018**.
19. Zhuang, W.; Li, S. (Eben); Zhang, X.; Kum, D.; Song, Z.; Yin, G.; Ju, F. *App. Energy*, **2020**, 262, 114553-114569. DOI: <https://doi.org/10.1016/j.apenergy.2020.114553>.
20. Kasimalla, V. K.; G., Naga-Srinivasulu; Velisala, V. *Int. J. Energy Res.* **2018**, 42, 4263-4283. DOI: <https://doi.org/10.1002/er.4166>.
21. Allaoua, B.; Asnoune, K.; Mebarki, B. *Int. J. Hydrogen Energy*. **2017**, 42, 21158-11166. DOI: <https://doi.org/10.1016/j.ijhydene.2017.06.209>.
22. Samsung SDI Co. Ltd. *Specification of product for Lithium-ion rechargeable cell model ICR18650-26F*. 2009. <https://datasheetspdf.com/datasheet/ICR18650-26F.html>. Accessed: 272 in February 2023.
23. Chen M.; Rincon-Mora, G. A. *IEEE Trans. Energy Convers.* **2006**, 21, 504-511. DOI: <https://doi.org/10.1109/TEC.2006.874229>.